Available online at www.sciencedirect.com
ScienceDirect
Solar Energy Materials & Solar Cells 91 (2007) 1765–1774
Solar Energy Materials and Solar Cells
www.elsevier.com/locate/solmat

Photoreduction of carbon dioxide with H_2 and H_2O over TiO_2 and ZrO_2 in a circulated photocatalytic reactor

Cho-Ching Lo[a], Chung-Hsuang Hung[b], Chung-Shin Yuan[a,*], Jen-Fong Wu[a]

[a]*Institute of Environmental Engineering, National Sun Yat-sen University, No. 70, Lian-Hai Road, Kaohsiung City, Taiwan, ROC*
[b]*Department of Safety, Health and Environmental Engineering, National Kaohsiung First University of Science and Technology, No. 1, University Street, Yanchau, Kaohsiung City, Taiwan, ROC*

Received 1 January 2007; received in revised form 1 June 2007; accepted 6 June 2007
Available online 20 July 2007

Abstract

The photocatalytic reduction of carbon dioxide (CO_2) was studied in a self-designed circulated photocatalytic reaction system under titanium dioxide (TiO_2, Degussa P-25) and zirconium oxide (ZrO_2) photocatalysts and reductants at room temperature and constant pressure. The wavelengths of incident ultraviolet (UV) light for the photocatalysis of TiO_2 and ZrO_2 were 365 and 254 nm, respectively. Experimental results indicated that the highest yield of the photoreduction of CO_2 were obtained using TiO_2 with H_2+H_2O and ZrO_2 with H_2. Photoreduction of CO_2 over TiO_2 with H_2+H_2O formed CH_4, CO, and C_2H_6 with the yield of 8.21, 0.28, and 0.20 μmol/g, respectively, while the photoreduction of CO_2 over ZrO_2 with H_2 formed CO at a yield of 1.24 μmol/g. The detected reaction products supported the proposition of two reaction pathways for the photoreduction of CO_2 over TiO_2 and ZrO_2 with H_2 and H_2O, respectively. Additionally, a one-site Langmuir–Hinshewood (L–H) kinetic model was successfully applied to simulate the photoreduction rate of CO_2.

Keywords: Photocatalytic reduction; Carbon dioxide; Operating parameters; Reaction pathways; Kinetic modeling

1. Introduction

Global warming caused by emissions of greenhouse gases such as carbon dioxide (CO_2), methane (CH_4), chlorofluorocarbons (CFCs), and nitrous oxide (N_2O) to the atmosphere, is widely regarded as one of the most severe environmental issues of recent years [1]. The atmospheric concentration of CO_2 has gradually increased mainly owing to human activities. Therefore, finding an effective solution to reduce the emission of CO_2 has attracted the interest of many researchers. The reduction of CO_2 by photocatalysts is one of the most promising methods since CO_2 can be reduced to useful compounds by irradiating it with UV light at room temperature and constant pressure [2–5].

Photocatalytic technology uses photosensitive semiconductor materials (such as TiO_2, ZrO_2, V_2O_5, ZnO, CeO_2, and NbO_5) as photocatalysts [6–12]. When such a semiconducting material is irradiated by light, whose energy exceeds its band-gap energy, e^-_{cb} in the semiconductor are promoted from the valence band to the conduction band, leaving h^+_{vb} in the valence band. The promoted e^-_{cb} and h^+_{vb} may participate in the succeeding oxidation and reduction reactions, respectively, with trapped species. The photocatalytic oxidation of organic pollutants to CO_2 has been extensively investigated [11–18]. The photocatalytic reduction of CO_2 to CO and hydrocarbons (such as CH_4, C_2H_6, HCHO, CH_3OH, and HCOOH) has attracted the interest of many researchers and investigators [19–29]. Most fundamental studies of the photocatalytic reduction of CO_2 have involved aqueous solutions [2,3,6,7,30–33]. The photoreduction rate of CO_2 is slow because of its low solubility and low utility of near-UV light [25].

In recent years, more attention has been paid to the photocatalytic reduction of gaseous CO_2. Previous

*Corresponding author. Tel.: +886 7 5252000x4409; fax: +886 7 5254409.
E-mail address: ycsngi@mail.nsysu.edu.tw (C.-S. Yuan).

0927-0248/$ - see front matter © 2007 Elsevier B.V. All rights reserved.
doi:10.1016/j.solmat.2007.06.003

investigations had focused primarily on the operating parameters of the photocatalytic reduction reaction, including the species of photocatalysts and reductants [19,20,26,32,34], the wavelength of illuminating light [25,27], the reaction temperature [22,27,29], and even the configuration of reactors [35]. Photocatalysts such as TiO_2, ZrO_2, ZnO and CdS have been investigated and, among them, TiO_2 is the most commonly used photocatalyst, because of its excellent photocatalytic activity and stability against photoirradiation [10,25,26,28,29,35,37,38]. Several researchers have reported that the photocatalytic reduction of CO_2 using gaseous H_2O acts on powdered TiO_2 at room temperature to form CO and CH_4 simultaneously [21,22,39]. When H_2 is used as a reductant, the photoreduction of CO_2 forms only CO [27]. Zirconium oxide (ZrO_2) is another semiconductor that has been widely applied in the heterogeneous photocatalytic reaction [25,26,29]. The energy of the band gap (E_g) for ZrO_2 is 5.0 eV, and the conduction band potential is −1.0 V versus a normal hydrogen electrode [34]. The relatively large E_g and the high conduction band potential allow ZrO_2 to be used as a photocatalyst in the photoreduction reaction [20,25,26,29]. Kohno et al. [25–29] also reported that ZrO_2, used as a photocatalyst, could reduce gaseous CO_2 with H_2 to form $HCOO^-$ and CO.

Previous studies on the photocatalytic reduction of CO_2 have performed the reaction mostly in batch photocatalytic reactors, which are generally associated with a relatively slow photoreduction of CO_2, and therefore, a longer reaction time. Yamagata et al. [35] investigated the employment of a closed-circulation photocatalytic reactor in the photoreduction of CO_2. Additionally, the circulated batch photocatalytic reactor has another two apparent advantages over the conventional batch photocatalytic reactor in overcoming the non-uniformity of the distribution of gas concentrations inside the reactor and shortening the reaction time. First, the circulated batch photocatalytic reactor provides a fairly high specific surface area on which the photocatalyst is immobilizing. Secondly, the distribution of gas concentrations in the reactor is relatively uniform. Both reduce the reaction time and thereby improve experimental quality.

In this study, a circulated photocatalytic reaction system was designed and employed to investigate the effects of operating parameters on the photoreduction of CO_2. The reaction pathways of CO_2 photoreduction were also studied by identifying the intermediates and products of the photoreduction reactions. Additionally, a one-site Langmuir–Hinshelwood (L–H) kinetic model of the photoreduction rate of CO_2 was further proposed.

2. Experimental methods

The circulated photocatalytic reaction system consisted of three major systems—the gas generation system, the photocatalytic reactor, and the sampling and analytic system. Fig. 1 schematically depicts the experimental setup. The experiments on the photocatalytic reduction of CO_2 were conducted using various photocatalysts and reductants. A gas stream of bottled hydrogen (H_2, 99.995%) was initially introduced to purge the circulatory system of gaseous matter. After the gaseous matter had been evacuated from the system, the valve was turned off until the carrier gas reached a pressure of 1.1 atm, and the diaphragm pump was then turned on to circulate the reaction gases. The gaseous reductants of appropriate concentrations (0.2%, 0.5%, 1.0%, 3.0% and 5.0%), obtained by mixing CO_2 (99.8%) (SUPELCO Scott Specialty Gases, Cat. No. 501298) with H_2 (99.995%), were injected into the photoreduction reaction system. Other reductants (H_2O, H_2+H_2O) were prepared by bubbling nitrogen (N_2, 99.995%) and/or H_2 into deionized water (D I water) to adjust the moisture content of the gas

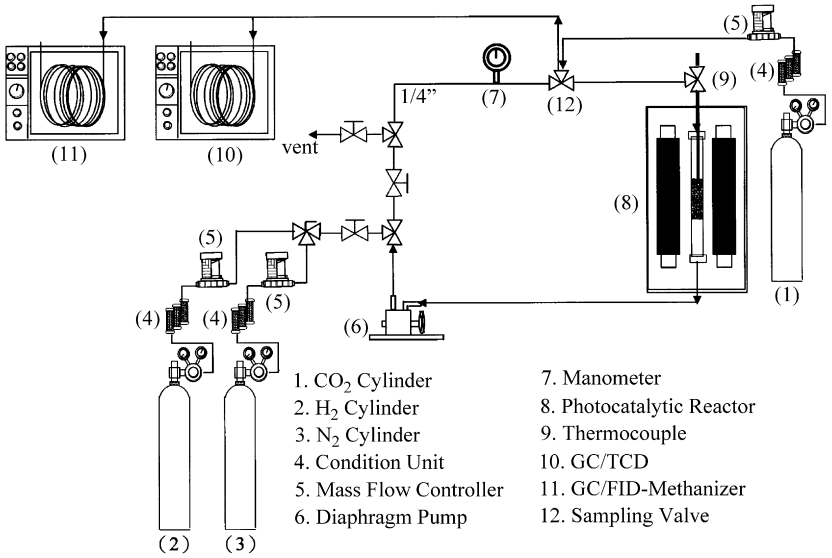

Fig. 1. Schematic of experimental setup.

stream, which was then measured using a hygrometer (General Eastern, Model M-2).

A packed-bed photocatalytic reactor (Fig. 2) was made from a quartz tube with a length of 480 mm and an internal diameter of 22.5 mm. Pyrex glass pellets (3.0 mm diameter) pre-immobilized with anatase titanium dioxide powder (TiO_2) (Degussa, P-25) or zirconium oxide powder (ZrO_2) (Prochem, 100 mesh) were packed inside the reactor as photocatalysts. The photocatalytic reactor was illuminated by four 15 W UV or near-UV lamps, as illustrated in Fig. 2. Two types of lamps tested herein were a near-UV fluorescent black lamp (Sankyo Denki Co. Ltd., Japan, F10TBLB 15 W) and a UV lamp (Sankyo Denki Co. Ltd., Japan, GL15, UV-C) with maximal spectral wavelengths of 365 and 254 nm, respectively. The intensity of UV radiation in the photocatalytic reactor was measured with a radiometer (UVP, Model UVX). The temperature inside the photocatalytic reactor was measured with a thermocouple (Shuan-Chang Electronic, Model CSM-321D) situated at the center of the photocatalytic reactor. The experiments were performed in an air-conditioned laboratory that ensured a stable indoor temperature. Although no particular effort was made to control the temperature inside the photocatalytic reactor, the temperature remained at $43 \pm 2\,^{\circ}C$ and did not vary much throughout the experiments. The reaction products in the outlet gas stream were analyzed as each experiment had approached its steady state.

Before anatase TiO_2 was immobilized on the Pyrex glass pellets, these glass pellets were etched in 5.0 M NaOH solution for 24 h at 100 °C. After they had been rinsed with D I water, the glass pellets were soaked in a 2.5% (W/W) Degussa P-25 TiO_2 slurry for 10–20 min, and were then baked in an oven at 105 °C for approximately 1 h. The thickness of the immobilized anatase TiO_2 layer on the surface of glass pellets was around 145 μm, which was equivalent to 14.8 mg of TiO_2 per g of glass pellets, and was estimated by dividing the mass of immobilized anatase TiO_2 by the bulk density of TiO_2 and the overall surface area of the glass pellets. The same procedure was also applied for the preparation of ZrO_2 immobilized glass pellets. Fig. 3 shows the flowchart of the preparation of the photocatalysts.

The reaction products in the outlet gas stream were further sampled by a gas-tight syringe and analyzed with two gas chromatographs. One gas chromatograph

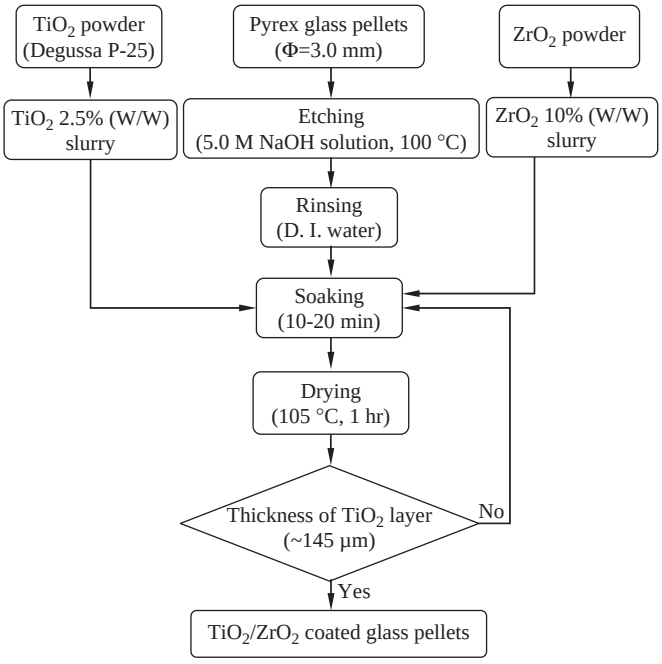

Fig. 3. Flowchart of photocatalyst preparation procedure.

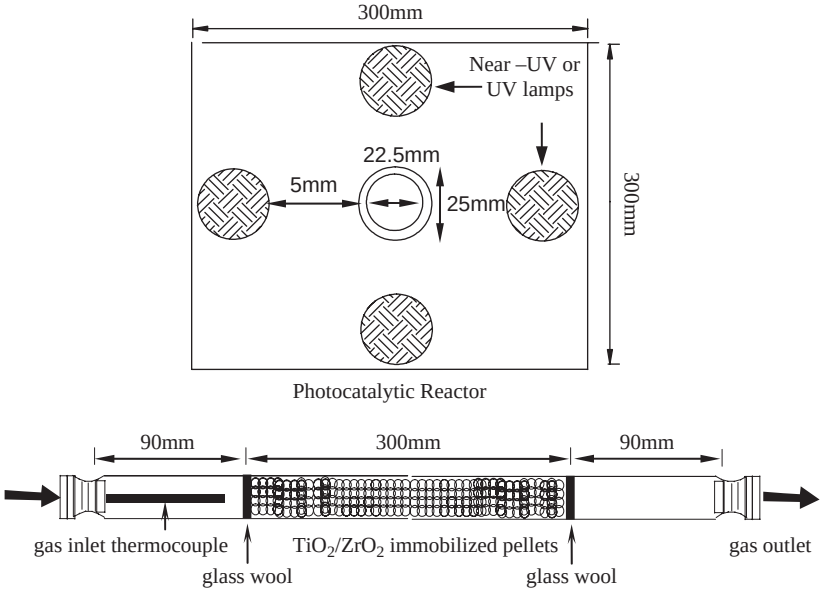

Fig. 2. Schematic of photocatalytic reactor.

with a thermal conductivity detector (GC/TCD) (HP, Model 4890 Series II) was used to analyze CH_4, C_2H_6, H_2 and H_2O, while another gas chromatograph with a flame-ionization detector followed by a methanizer (GC/FID-Methanizer) (HP, Model 6890 Series) was used to determine the concentrations of CO and CO_2. The separation column in the GC/TCD was a 50/80 Porapak R column (SUPELCO, 8 ft × 1/8 in S S). That in the GC/FID-methanizer was an HP-PLOT Q column (HP, 15 m × 0.32 mm × 20.0 μm film thickness).

3. Results and discussion

In this study, the photoreduction of CO_2 was conducted in the circulated photocatalytic reaction system to investigate the influence of the operating parameters on the photoreduction of CO_2. The tested photocatalysts were TiO_2 and ZrO_2, and the wavelengths of UV light were 365 and 254 nm, respectively. Other operating parameters included the species of the reductants (H_2, H_2O and H_2+H_2O) and the initial CO_2 concentration (0.2%, 0.5%, 1.0%, 3.0% and 5.0%).

3.1. Effects of reductants

3.1.1. TiO_2 as photocatalyst

Fig. 4 illustrates the effects of the reductant on the yield of the products of CO_2 photoreduction. The reaction products varied markedly with the species of reductant used. The photocatalytic reduction of CO_2 over TiO_2 with H_2 formed CH_4, CO and C_2H_6 with the yield s of 2.91, 0.12 and 0.14 μmol/g, respectively. The photoreduction of CO_2 with H_2O formed CH_4 and CO with the yield of 3.28 and 0.21 μmol/g, respectively. However, C_2H_6 was not observed in this case. The photoreduction of CO_2 with H_2+H_2O formed CH_4, CO, and C_2H_6 with the yield of 8.21, 0.28 and 0.20 μmol/g, respectively. The yield of CH_4 and CO with H_2O exceeded those with H_2. However, the yield of CH_4, CO and C_2H_6 with H_2+H_2O markedly exceeded those with either H_2 or H_2O, being almost the sum of those obtained using H_2 and H_2O.

Hydrogen is an important reductant and has been widely employed in photoreduction studies. Hydrogen molecules can be adsorbed dissociatively to form H^+ on the surface of TiO_2 and supplied as a hydrogen atom to convert CO_2 to hydrocarbons by photoreduction [33,35]. Subrahmanyam et al. [33] reported that H^+ would further react with e^-_{cb} to produce $^\bullet H$ radicals. The $^\bullet H$ radicals are highly reactive species, which directly react with CO_2 and accelerate its reduction. The photocatalytic pathways of H_2 are written as follows. These reactions convert CO_2 to CH_4:

$$TiO_2 + h\nu \rightarrow h^+_{vb} + e^-_{cb}, \quad (1)$$

$$H_2 \rightarrow 2H^+ + 2e^-_{cb}, \quad (2)$$

$$H^+ + e^-_{cb} \rightarrow {}^\bullet H, \quad (3)$$

$$CO_2 + 8e^-_{cb} + 8\,{}^\bullet H \rightarrow CH_4 + 2H_2O. \quad (4)$$

Adsorbed H_2 may also directly react with active carbonate species, such as the $^\bullet CO_2^-$ radical [25,27]. Generally, CO_2 acts as an e^-_{cb} accepter in the conduction band in the photocatalytic reduction of CO_2. When adsorbed CO_2 accepts an e^-_{cb}, it becomes the $^\bullet CO_2^-$ radical. Kohno et al. [27] reported that two $^\bullet CO_2^-$ radicals may produce CO and carbonate (CO_3^{2-}) in the photoreduction of CO_2 with hydrogen over Rh/TiO_2. Water is another important species that is added as a reactant in photocatalytic reduction [20,22]. The photocatalytic reaction of H_2O proceeds as follows:

$$H_2O + h^+_{vb} \rightarrow {}^\bullet OH + H^+. \quad (5)$$

The efficiency of photocatalysis depends upon the lifetime of the e^-_{cb} and h^+_{vb}. If no suitable reactant accepts e^-_{cb} or catches h^+_{vb} on the photocatalyst (TiO_2), then the e^-_{cb} and h^+_{vb} recombine and release heat, reducing the photocatalytic reaction rate. Water, as one of the chemical species that catches the h^+_{vb}, has been widely used in many photocatalytic oxidation and reduction studies [20,22]. In this work, the addition of water accelerated the photoreduction of CO_2 over TiO_2 with H_2. The quantities of all products (CH_4, C_2H_6 and CO) increased markedly as water was added. Accordingly, adding water to the photoreduction reaction system is proposed not to have changed the reaction pathways, but to have accelerated the photoreduction of CO_2 with H_2, since water donated e^-_{cb} to inhibit the recombination of e^-_{cb} and h^+_{vb}. Moreover, the dissociation of H^+ from water might also supply more hydrogen atoms for the photoreduction of CO_2. This study also revealed that the amount of products of the photoreduction of CO_2 with H_2+H_2O was almost the sum of the amounts of H_2O and H_2. The results indicated that adding H_2O and H_2 as reductants markedly accelerated the reaction. No obvious competition between H_2 and H_2O for the photoreduction of CO_2 over TiO_2 was observed. Thus, in this study, the most effective reductants that enhanced the photoreduction of CO_2 were H_2+H_2O over TiO_2, and the yield of CH_4, CO and C_2H_6 were 8.21, 0.28 and 0.20 μmol/g, respectively.

3.1.2. ZrO_2 as photocatalyst

Using ZrO_2 as a photocatalyst in the photoreduction of CO_2 with H_2 formed only CO with a yield of approximately 1.24 μmol/g. The results concurred with those obtained by Kohno et al. [25–28]. Similar results were observed for the photoreduction of CO_2 with H_2O and H_2+H_2O, and their yields were 0.08 and 1.02 μmol/g, respectively. The yield of CO for the photoreduction of CO_2 with H_2+H_2O was higher than that with either H_2 or H_2O. The details of the interaction of CO_2 with H_2 over ZrO_2 are not yet clear. Kohno et al. [26] employed electron paramagnetic resonance (EPR) technology to study the mechanism of the photoreduction of CO_2 over ZrO_2 with H_2, and reported that no dissociation of H_2 was

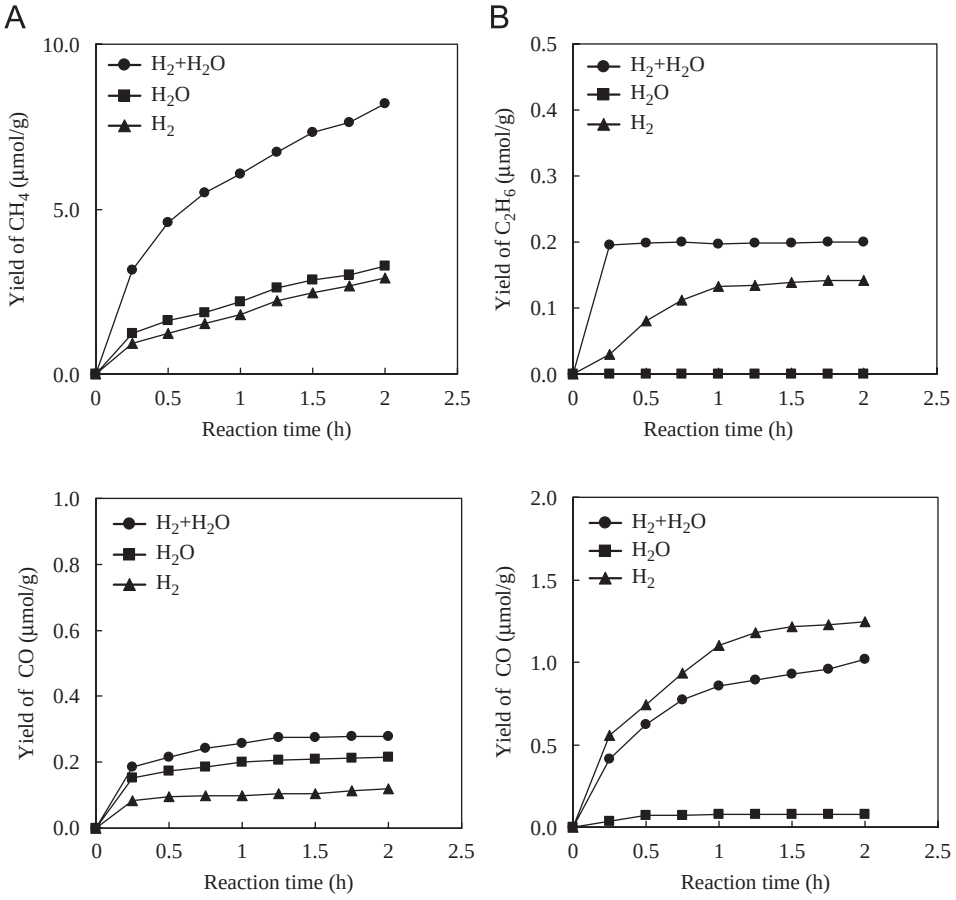

Fig. 4. Effects of reductants on the yield of reaction products. ($[CO_2] = 5.0\%$; temperature $= 43 \pm 2\,^{\circ}C$; pressure $= 1.1$ atm; (A) TiO_2 loading $= 0.25$ g, UV wavelength at 365 nm; (B) ZrO_2 loading $= 0.25$ g, UV wavelength at 254 nm).

observed on the ZrO_2 surface, since infrared adsorption bands of Zr–H were not detected at reaction temperatures lower than 673 K. They hypothesized that H_2 did not have to be dissociated and photoexcited to form H^+ and/or $^{\bullet}H$ radicals over ZrO_2 in order to participate in the photoreduction reaction. Furthermore, they claimed that CO_2 adsorbed on the ZrO_2 surface could be photoexcited to form $^{\bullet}CO_2^-$ radicals, as evidenced by EPR. The $^{\bullet}CO_2^-$ radical was stable and had a long lifetime in the dark reaction. Adding H_2 to react with $^{\bullet}CO_2^-$ radicals in the dark reduced the $^{\bullet}CO_2^-$ lifetime, indicating that the reaction between H_2 and $^{\bullet}CO_2^-$ could occur in the absence of irradiation.

In this work, the highest CO yield of 1.24 μmol/g was observed for the photoreduction of CO_2 over ZrO_2 with H_2. The addition of H_2O induced the reaction of CO_2, indicating that H^+ and/or $^{\bullet}H$ radicals formed from H_2O did not accelerate the photoreduction of CO_2 over ZrO_2. Water molecules competed with H_2 for the reactive sites on the surface of ZrO_2.

3.2. Effects of initial CO_2 concentration

Fig. 5 illustrates the influence of initial CO_2 concentration on the yield of the reaction products of the photoreduction of CO_2 with various photocatalysts and reductants. For the photoreduction of 5.0% CO_2 over TiO_2 with $H_2 + H_2O$, the yield of CH_4, C_2H_6, and CO were 8.21, 0.20 and 0.28 μmol/g, respectively. For initial concentrations of 0.2% and 0.5% CO_2 over TiO_2 with $H_2 + H_2O$, CH_4 was the only product and the yield was 0.59 and 1.31 μmol/g, respectively. Similar results were observed for the photoreduction of 5.0% CO_2 using TiO_2 with H_2 and the yields of CH_4 were 2.91 μmol/g. The results indicated that high initial concentration of CO_2 enhanced the formation of CH_4 and CO with various reductants. However, only CH_4 was formed at low initial CO_2 concentrations. Additionally, similar results were observed for the photoreduction of CO_2 over TiO_2 using H_2 as the reductant.

When ZrO_2 was used as the photocatalyst, the yield of CO were 1.02 and 1.24 μmol/g for the photoreduction of 5.0% CO_2 with $H_2 + H_2O$ and H_2, respectively. However, for the photoreduction of 0.5% CO_2 with $H_2 + H_2O$, a lower CO yield of 0.13 μmol/g was observed. Experimental results indicated that higher initial CO_2 concentration could result in higher concentration of CO produced when ZrO_2 was used with $H_2 + H_2O$.

3.3. Comparison with previous results

Table 1 compares the product yield obtained herein with those in other studies. When TiO_2 was used as the

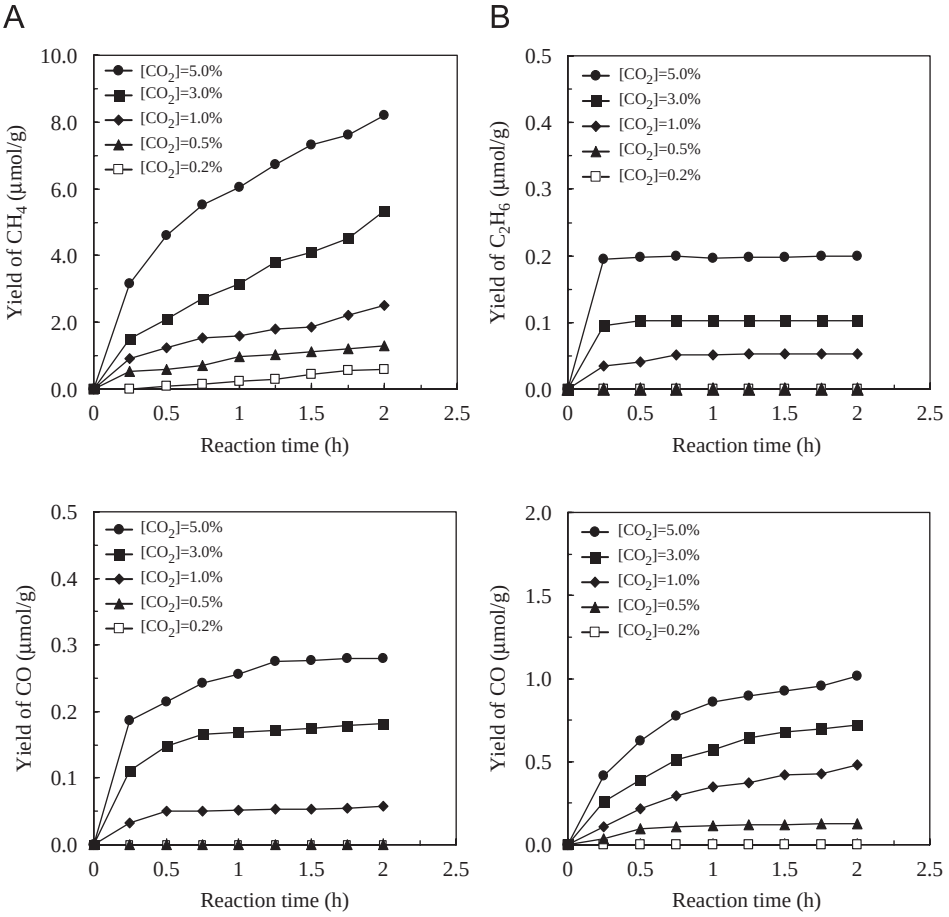

Fig. 5. Effects of initial CO_2 concentrations on the yield of reaction products (reductants = $H_2 + H_2O$; temperature = 43 ± 2 °C; pressure = 1.1 atm; (A) TiO_2 loading = 0.25 g, UV wavelength at 365 nm; (B) ZrO_2 loading = 0.25 g, UV wavelength at 254 nm).

photocatalyst in the photoreduction of CO_2 with H_2, the observations of the major product CH_4, in this study, were consistent with those of Anpo et al. [20]. This study also revealed that the formation of CO and C_2H_6, which did not occur in Anpo's work, although the yields of CO and C_2H_6 were approximately 1/10th–1/20th that of CH_4 (Fig. 4). The yield of CH_4 herein (4.11 μmol/gh) was 13.7 times higher than that of Anpo's (0.30 μmol/gh) (Table 1). When ZrO_2 was used as the photocatalyst, CO was the only product observed in this study and in Kohno's study [25,29]. The yield of CO herein (0.51 μmol/gh) was approximately that of Kohno's (0.70 μmol/gh) (Table 1). Although the yields of product were relatively low, the photoreduction of CO_2 to form CO, CH_4 and C_2H_6 at room temperature was proven to be feasible. Further investigation on the enhancement of the photoreduction rate of CO_2 will be conducted in the future study.

3.4. Reaction pathways of CO_2 photoreduction

Based on the experimental results obtained herein and elsewhere, reaction pathways are proposed to describe the photoreduction reaction of CO_2 for various photocatalysts and reductants, as shown in Fig. 6.

3.4.1. TiO_2 as photocatalyst

When TiO_2 was used as the photocatalyst, no reaction product of the photoreduction of CO_2 was observed without the use of a reductant (either H_2 or H_2O). However, adding H_2 and/or H_2O as reductant(s) would effectively enhance the photoreduction of CO_2. The results indicated that the photoreduction of CO_2 could proceed in the presence of $^{\bullet}H$ radicals from either H_2 or H_2O. When H_2 was used as the reductant, the major product was CH_4, and only a little CO and C_2H_6 were formed. The amount of CH_4 produced increased constantly, while the amounts of CO and C_2H_6 tended to level off with reaction time.

The mechanisms of the photoreduction of CO_2 remain unclear so far. Subrahmanyam et al. [33] reported that CH_4 could be formed in a reaction of eight highly reactive $^{\bullet}H$ radicals reacting with CO_2. Fig. 6(A) shows a possible reaction pathway for the photoreduction of CO_2 with H_2. Furthermore, the combination of two $^{\bullet}CH_3$ radicals may form C_2H_6. In this work, the yield of CH_4 increased with reaction time almost constantly, suggesting that TiO_2 could be used in the photoreduction of CO_2. The reactivity of TiO_2 did not detectably decay during the experiments. C_2H_6 may be reduced back to CH_4 by reacting with $^{\bullet}H$

Table 1
Comparison of products yield obtained from this study with other results

Photocatalysts	Operating parameters	Products yield	References
TiO_2	CO_2: 5% H_2: 90% H_2O: 5% 4 × 15 W near-UV lamp[a]	CH_4: 4.11 μmol/g h CO: 0.14 μmol/g h C_2H_6: 0.10 μmol/g h	This study
TiO_2	CO_2: 150 μmol H_2: 50 μmol 500 W near-UV lamp[a]	CH_4: 0.30 μmol/g h	Anpo (1998)
ZrO_2	CO_2: 5% H_2: 95% 4 × 15 W near-UV lamp[b]	CO: 0.51 μmol/g h	This study
ZrO_2	CO_2: 150 μmol H_2: 50 μmol 500 W near-UV lamp[b]	CO: 0.70 μmol/g h	Kohno (1997)

[a]Ultra-low-pressure mercury lamp ($\lambda = 365$ nm).
[b]Ultra-low-pressure mercury lamp ($\lambda = 254$ nm).

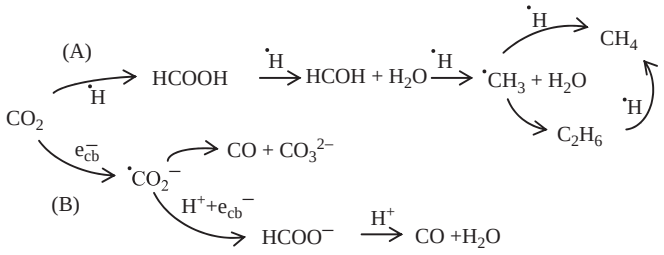

Fig. 6. Reaction pathways of CO_2 photoreduction.

radicals, since the yield of C_2H_6 remained nearly constant with reaction time (Fig. 4).

Another pathway for the photoreduction of CO_2 was the formation of $^{\bullet}CO_2^-$ radicals from CO_2 [27]. Kohno et al. [27] reported that two $^{\bullet}CO_2^-$ radicals could form CO and carbonate (CO_3^{2-}) for the photoreduction of CO_2 over Rh/TiO_2 with H_2. Kaneco et al. [25] revealed that $^{\bullet}CO_2^-$ radicals could react with H^+ and e_{cb}^- to form formic acid (HCOOH) in the liquid-phase photoreduction of CO_2 over TiO_2. Liu et al. [36] proposed the possibility of the formation of CO in a reaction of formate ion ($HCOO^-$) with $^{\bullet}CO_2^-$ and e_{cb}^-. As shown in Fig. 6(B), this study proposed that carbon dioxide (CO_2) could initially react with e_{cb}^- to form radical $^{\bullet}CO_2^-$ on the surface of photocatalysts. Afterward, radical $^{\bullet}CO_2^-$ could react with H^+ and e_{cb}^- to form $HCOO^-$, and further react with H^+ to form CO and H_2O. Herein, e_{cb}^- and H^+ were formed from two typical photocatalytic reactions, $TiO_2 + h\nu \rightarrow h_{vb}^+ + e_{cb}^-$ and $H_2 \rightarrow 2H^+ + 2e_{cb}^-$ (Eqs. (1) and (2)).

3.4.2. ZrO_2 as photocatalyst

The reaction pathways for the photoreduction of CO_2 over ZrO_2 are simpler than over TiO_2. As mentioned above, the only reaction product was CO, and the main pathway for forming CO was the reaction between $^{\bullet}CO_2^-$ radicals and H_2; no reaction could occur among CO_2, H^+ and $^{\bullet}H$ radicals. Previous investigators found, using infrared spectroscopy, that formate ions were formed over ZrO_2 with H_2, and proposed that the formate ion was an intermediate that served as a reductant of another CO_2 molecule [27]. Fig. 6(B) shows the reaction scheme proposed in this study.

3.5. Kinetic modeling of CO_2 photoreduction

A one-site Langmuir–Hinshewood (L–H) kinetic model was further applied to simulate the photoreduction rate of CO_2 over TiO_2, during the photoreduction of CO_2. Based on the assumption that the reaction takes place only on the external surface of TiO_2, the isothermal operation of the cylindrical photocatalytic reactor system employed in this study can be modeled. The L–H kinetic model is expressed as follows [14,16,37,40];

$$r = -\frac{dC}{dt} = -k_{LH}\frac{KC}{1+KC}, \tag{6}$$

where C is the concentration of CO_2 (ppm); k_{LH} is the reaction rate constant of CO_2 photoreduction (ppm/h); K is the adsorption equilibrium constant of CO_2 (1/ppm); and t is the reaction time (h). Integrating and rearranging Eq. (6) gives,

$$\ln\left(\frac{C}{C_0}\right) = K(C_0 - C) - k_{LH}Kt. \tag{7}$$

The experimental results obtained with various initial CO_2 concentrations at a constant detention time yield a plot of $\ln(C/C_0)$ vs. $(C_0–C)$, from which the reaction rate

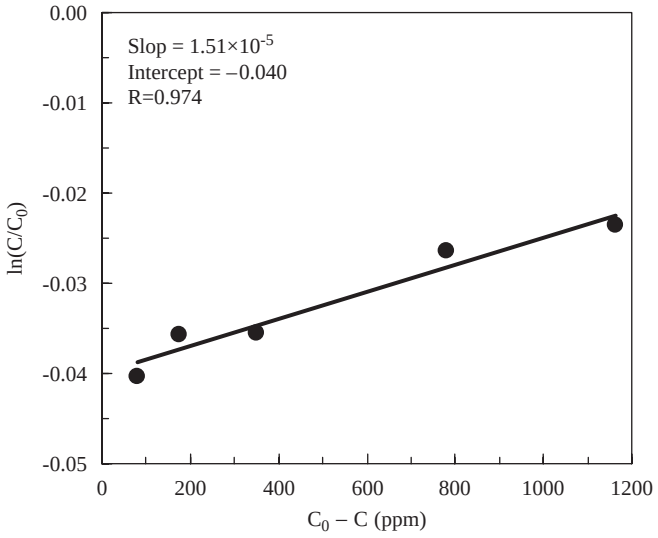

Fig. 7. Kinetic regression for photoreduction of CO_2 conducted at retention time of 2 h (reductant = H_2+H_2O; temperature = 43±2 °C; pressure = 1.1 atm).

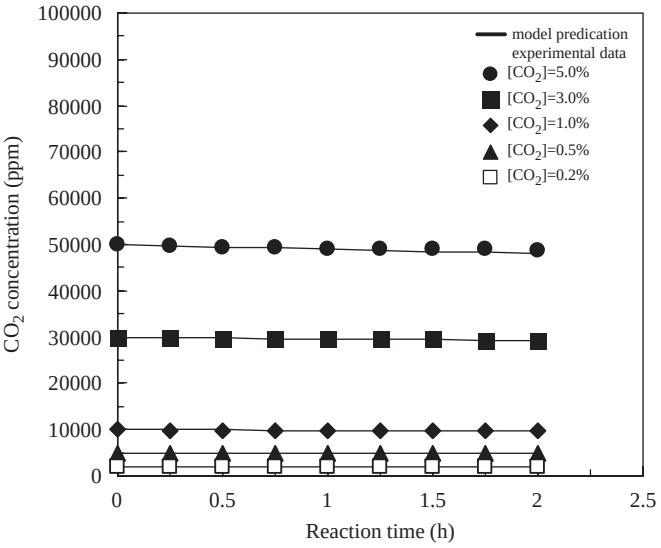

Fig. 8. Calculated and initial CO_2 concentrations for the photoreduction of CO_2 with various reaction times (reductant = H_2+H_2O; temperature = 43±2 °C; pressure = 1.1 atm).

constant (k_{LH}) and the adsorption equilibrium constant (K) can be determined, as shown in Fig. 7, for experiments conducted at the detention time of 2 h. In this study, the k_{LH} and K values were determined to be 1325 ppm/h and 1.51×10^{-5} 1/ppm, respectively, by comparing experimental data with the outputs of the L–H kinetic model. The rate of reduction of CO_2 in the photoreduction of CO_2 over TiO_2 can be expressed by

$$r = -\frac{dC}{dt} = -\frac{2.00\times10^{-2}\,C}{1+1.51\times10^{-5}\,C}. \quad (8)$$

Fig. 8 plots and compares the photoreduction rates of CO_2 by Eq. (8) with the experimental data. For the

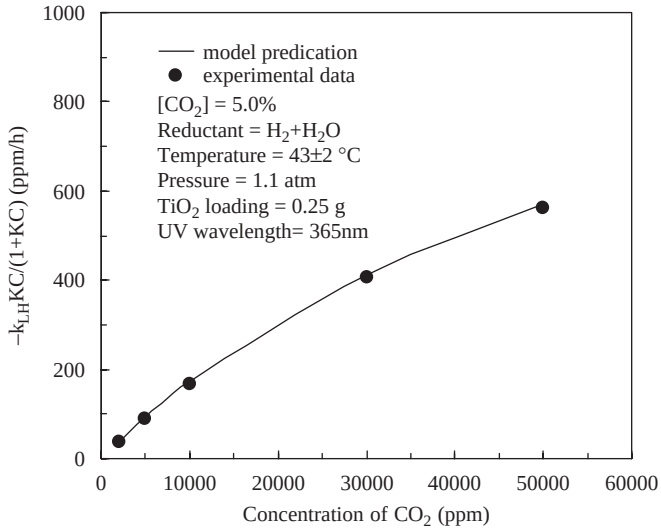

Fig. 9. Calculated and reaction rates for the photoreduction of CO_2 with various initial concentration (reductant = H_2+H_2O; temperature = 43±2 °C; pressure = 1.1 atm).

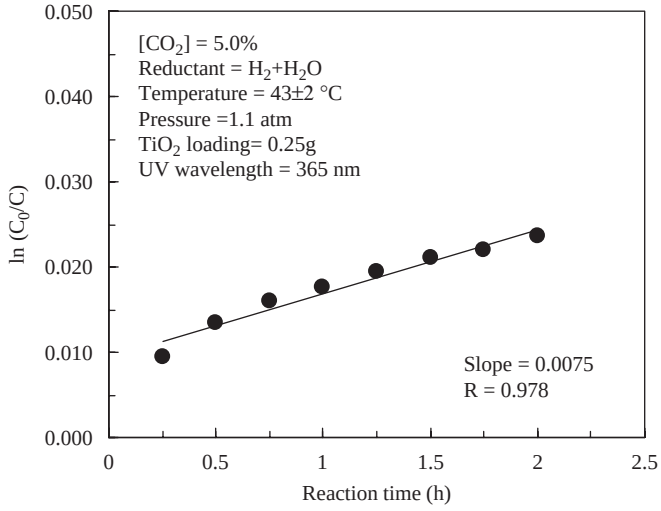

Fig. 10. Reaction rate regression for the photoreduction of CO_2 with various reaction times.

experiments conducted with initial CO_2 concentrations ranging from 0.2% to 5.0% (2000–50,000 ppm), the temporal behavior of the photocatalytic reduction of CO_2 is given effectively by Eq. (8). The data from experiments undertaken at the reaction of 2 h with various initial CO_2 concentrations from 0.2% to 5.0%, yielded similar trends, as shown in Fig. 9. Basically, model predictions agreed very well with the experimental results, as shown in Figs. 7–9.

Experimental results of the CO_2 photoreduction with various retention times were in the range of 0.25–2 h. Fig. 10 summarizes these data and presents the kinetic regression results. The photoreduction of CO_2 can be simulated by the pseudo-first-order reaction, whose rate constant was close to the regressed rate constant obtained from the following discussion about the effect of CO_2 concentration. Fig. 11 shows that the photoreduction rate

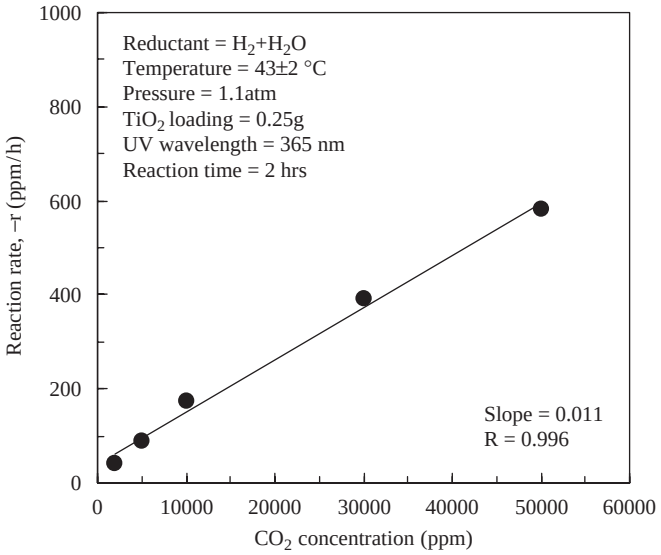

Fig. 11. Reaction rate for the photoreduction of CO_2 with various initial CO_2 concentration.

constants of CO_2 were 0.0126 and 0.0075 1/h, for the experiments conducted with 0.2% and 5.0% of CO_2, respectively. The photoreduction rate of CO_2 increased linearly with the initial CO_2 concentration, indicating a pseudo-first-order relationship and suggesting that the adsorption of CO_2 on TiO_2 is the rate-determining step. Liu et al. [36] also indicated that surface adsorption was predominant during the photoreduction of CO_2 using modified CdS photocatalysts.

4. Conclusions

Experimental results obtained from the UV/TiO_2 photocatalytic reduction of CO_2 at room temperature and constant pressure indicated that the most effective reductant for the photoreduction of CO_2 was H_2 using both TiO_2 and ZrO_2 photocatalysts. The highest yield rates of CO_2 photoreduction were obtained when H_2 and saturated water vapor (H_2O) were used for TiO_2 and only H_2 was used for ZrO_2. The photocatalytic reduction of CO_2 with H_2 and H_2O for TiO_2 formed CO, CH_4 and C_2H_6. The use of ZrO_2 as the photocatalyst for the photoreduction of CO_2 with H_2 formed only CO. Two major reaction pathways for the photoreduction of CO_2 were proposed in this study. One pathway described the photoreduction reactions when H_2 was used over TiO_2 to form CO, CH_4, and C_2H_6. However, the photoreduction of CO_2 using H_2O over TiO_2 formed CO and CH_4. The other pathway described the photoreduction reaction of CO_2 using various reductants over ZrO_2, forming only CO. The photoreduction rate of CO_2 increased linearly with the increasing initial CO_2 concentration. A one-site Langmuir–Hinshewood kinetic model can be successfully applied to simulate the photoreduction rate of CO_2 during the photoreduction of CO_2. Although the photoreduction rate of CO_2 and the yield of reaction products were relatively low, this innovative technology was still valuable for future development. Further investigation is required for enhancing the photoreduction rate of CO_2 by using more efficient photocatalysts and/or reductants.

Acknowledgments

The authors thank the Environmental Protection Administration of Taiwan for financially supporting this research under Contract no. EPA-90-FA17-03-043.

References

[1] M. Takeuchi, Y. Sakamoto, S. Niwa, Sci. Total Environ. 277 (2001) 15.
[2] Z. Goren, I. Willner, A.J. Nelson, A.J. Frank, J. Phys. Chem. 94 (1990) 3784.
[3] K. Hirano, K. Inoue, T. Yatsu, J. Photochem. Photobiol. A 64 (1992) 255.
[4] O. Ishitani, C. Inoue, Y. Suzuki, T. Ibusuki, J. Photochem. Photobiol. A 72 (1993) 269.
[5] H. Uchida, T. Sasaki, K. Ogura, J. Mol. Catal. 93 (1994) 269.
[6] T. Inoue, A. Fujishima, S. Konishi, K. Honda, Nature 277 (1979) 637.
[7] H. Inoue, H. Moriwaki, K. Maeda, H. Yoneyama, J. Photochem. Photobiol. A 86 (1995) 191.
[8] K. Nikolaou, Sci. Total Environ. 235 (1999) 71.
[9] I.H. Tseng, W.H. Chang, C.S. Jeffrey Wu, Appl. Catal. B 37 (2002) 37.
[10] G. Silvia Botta, A. José Navío, C. María Hidalgo, M. Gloria Restrepo, I. Marta Litter, J. Photochem. Photobiol. A 129 (1999) 89.
[11] C.H. Hung, B.J. Marinas, Environ. Sci. Technol. 31 (1997) 562.
[12] C.H. Hung, B.J. Marinas, Environ. Sci. Technol. 31 (1997) 1440.
[13] W.F. Jardim, R.M. Alberici, Appl. Catal. B 14 (1997) 55.
[14] K.H. Wang, H.H. Tsai, Y.H. Hsieh, Appl. Catal. B 17 (1998) 313.
[15] C.S. Yuan, C.H. Hung, J. Chin. Inst. Eng. 8 (1998) 11.
[16] W. Wang, Y. Ku, J. Photochem. Photobiol. A 159 (2003) 47.
[17] K. Hanna, C. Brauer, P. Germain, J.M. Chovelon, C. Ferronato, Sci. Total Environ. 332 (2004) 51.
[18] A. Strini, S. Cassese, L. Schiavi, Appl. Catal. B 61 (2005) 90.
[19] M. Anpo, H. Yamashita, Y. Ichihashi, S. Ehara, J. Electroanal. Chem. 396 (1995) 21.
[20] M. Anpo, H. Yamashita, K. Ikeue, Y. Fujii, S.G. Zhang, Y. Ichihashi, D.R. Park, Y. Suzuki, K. Koyano, T. Tatsumi, Catal. Today 44 (1998) 327.
[21] F. Saladin, L. Forss, I. Kamber, J. Chem. Soc. Chem. Commun. (1995) 533.
[22] F. Saladin, I. Alxneit, J. Chem. Soc. Faraday Trans. 93 (1997) 41594163.
[23] J. Premkumar, R. Ramaraj, J. Photochem. Photobiol. A 110 (1997) 53.
[24] P. Johne, H. Kisch, J. Photochem. Photobiol. A 111 (1997) 223.
[25] Y. Kohno, T. Tanaka, T. Funabiki, S. Yoshida, Chem. Commun. (1997) 841.
[26] Y. Kohno, T. Tanaka, T. Funabiki, S. Yoshida, J. Chem. Soc. Faraday Trans. 94 (1998) 1875.
[27] Y. Kohno, H. Hayashi, S. Takenaka, T. Tanaka, T. Funabiki, S. Yoshida, J. Photochem. Photobiol. A 126 (1999) 117.
[28] Y. Kohno, T. Tanaka, T. Funabiki, S. Yoshida, Phys. Chem. Chem. Phys. 2 (2000) 5302.
[29] Y. Kohno, T. Tanaka, T. Funabiki, S. Yoshida, Phys. Chem. Chem. Phys. 2 (2000) 2635.
[30] H. Hori, O. Ishitani, K. Koike, P.A. Frank Johnson, T. Ibusuki, Energy Convers. Manage. 36 (1995) 621.
[31] H. Yoneyama, Catal. Today 39 (1997) 169.
[32] S. Kaneco, H. Kurimoto, K. Ohta, T. Mizuno, A. Saji, J. Photochem. Photobiol. A 109 (1997) 59.

[33] M. Subrahmanyam, S. Kaneco, N. Alonso-Vante, Appl. Catal. B 23 (1999) 169.
[34] K. Sayama, H. Arakawa, J. Phys. Chem. 97 (1993) 531.
[35] S. Yamagata, M. Nishijo, N. Murao, S. Ohta, I. Mizoguchi, Zeolites 15 (1995) 490.
[36] B.J. Liu, T. Torimoto, H. Yoneyama, J. Photochem. Photobiol. A 113 (1998) 93.
[37] M.R. Nimlos, E.J. Wolfrum, M.L. Brewer, J.A. Fennell, G.B. Bintner, Environ. Sci. Technol. 30 (1996) 3102.
[38] C.H. Hung, R.M. Lai, J.F. Wu, J. Chin. Inst. Eng. 15 (2005) 153.
[39] C.C. Lo, Y.L. Hung, J.F. Wu, C.S. Yuan, C.H. Hung, Y.C. Wu, J. Chin. Inst. Eng. 15 (2005) 143.
[40] J.F. Wu, C.H. Hung, C.S. Yuan, J. Photochem. Photobiol. A 170 (2005) 299.